Cell Calcium (1998) **24**(2), 87–96

Functional measurements of $[Ca^{2+}]$ in the endoplasmic reticulum using a herpes virus to deliver targeted aequorin

Maria Teresa Alonso, Maria Jose Barrero, Estela Carnicero, Mayte Montero, Javier Garcia-Sancho, Javier Alvarez

Departamento de Bioquímica y Biología Molecular y Fisiología, Instituto de Biologia y Genetica Molecular (IBGM), Facultad de Medicina, Universidad de Valladolid y CSIC, Valladolid, Spain

Summary Changes in the free calcium concentration of the endoplasmic reticulum ($[Ca^{2+}]_{er}$) play a central role controlling cellular functions like contraction, secretion or neuronal signaling. We recently reported that recombinant aequorin targeted to the endoplasmic reticulum (ER) [Montero M., Brini M., Marsault R. et al. Monitoring dynamic changes in free Ca^{2+} concentration in the endoplasmic reticulum of intact cells. *EMBO J* 1995; **14**: 5467—5475, Montero M., Barrero M.J., Alvarez J. $[Ca^{2+}]$ microdomains control agonist-induced Ca^{2+} release in intact cells. *FASEB J* 1997; **11**: 881—886] can be used to monitor selectively $[Ca^{2+}]_{er}$ in intact HeLa cells. Here we have used a herpes simplex virus type 1 (HSV-1) based system to deliver targeted aequorin into a number of different cell types including both postmitotic primary cells (anterior pituitary cells, chromaffin cells and cerebellar neurons) and cell lines (HeLa, NIH3T3, GH_3 and PC12 cells). Functional studies showed that the steady state lumenal $[Ca^{2+}]_{er}$ ranged from around 300 μM in granule cells to 800 μM in GH_3 cells. $InsP_3$-coupled receptor stimulation with agonists like histamine (in HeLa, NIH3T3 and chromaffin cells), UTP and bradykinin (in PC12 cells) or thyrotropin-releasing hormone (TRH, in GH_3 cells) produced a very rapid decrease in lumenal $[Ca^{2+}]_{er}$. Caffeine caused a rapid Ca^{2+} depletion of the ER in chromaffin cells, but not in the other cell types. Depolarization by high K^+ produced an immediate and reversible increase of $[Ca^{2+}]_{er}$ in all the excitable cells (anterior pituitary, GH_3, chromaffin cells and granule neurons). We conclude that delivery of recombinant aequorin to the ER using HSV amplicon provides the first direct quantitative and dynamic measurements of $[Ca^{2+}]_{er}$ in several primary non-dividing cells.

INTRODUCTION

Changes in the concentration of cytosolic Ca^{2+} ($[Ca^{2+}]_c$) are known to regulate many physiological responses to different extracellular stimuli, both in excitable and non-excitable cells. Receptor stimulation can lead to a variety of complex spatiotemporal patterns of increases in $[Ca^{2+}]_c$ like Ca^{2+} waves and Ca^{2+} oscillations. The mechanisms for Ca^{2+} release from the ER, for Ca^{2+} entry across the plasma membrane, and for sequestering released Ca^{2+} underlie these complex responses [3–5]. The ER, or some of its subcompartments, is believed to be the major cellular Ca^{2+} store, releasing Ca^{2+} upon stimulation of $InsP_3$-coupled plasma membrane receptors or via Ca^{2+}-induced Ca^{2+}-release (CICR), to cause rises in $[Ca^{2+}]_c$ [6]. However, in spite of efforts focused on studying the different components of calcium signaling, direct and specific measurement of $[Ca^{2+}]$ inside the ER of intact cells has been a difficult task. Recently, the cloning of the gene encoding for the photoprotein aequorin has allowed

Received 5 March 1998
Revised 12 June 1998
Accepted 16 June 1998

Correspondence to: Dr Maria Teresa Alonso, Departamento de Bioquímica y Biología Molecular y Fisiología, Facultad de Medicina, Universidad de Valladolid, 47005 Valladolid, Spain
Tel: +34 983 423085; Fax: +34 983 423588
E-mail: talonso@cpd.uva.es

its expression in mammalian cell cultures. Furthermore, the aequorin gene has been modified by including defined targeting signals. Thus, a number of aequorin chimeras targeted to different subcellular compartments such as mitochondria [7], the nucleoplasm [8], cytosol [9], ER [1,10,11] and sarcoplasmic reticulum [12] have been generated. The targeting strategy was fully successful in every case, but measurement of $[Ca^{2+}]_{er}$ was particularly difficult because of the high $[Ca^{2+}]$ in that compartment, which produced a rapid consumption of aequorin [1,13]. We recently solved this problem by using coelenterazine n, a modified form of the prosthetic group of aequorin which reduces the rate of luminescence and allows the performance of long-lasting measurements of $[Ca^{2+}]_{er}$ in intact cells [2,14]. However, although the use of these chimeras has represented a landmark in the field of subcellular $[Ca^{2+}]$ investigation, most studies have been performed in one particular cell line (HeLa). This restriction is due to the difficulty in introducing plasmid DNA into primary postmitotic cells by non-viral methods such as Ca^{2+} phosphate, electroporation or liposomes. To overcome this limitation, we decided to develop a delivery system capable of directing the expression of ER-targeted aequorin in different cell types and particularly in primary cells, the most interesting ones from a physiological point of view.

Herpes simplex virus type 1 (HSV-1) is a neurotropic virus with many unique features that make it suitable as a gene transfer vector for mammalian cells, both in vitro and in vivo [15]. Its characteristics include wide host cell range, efficient infection, ability to deliver genes to both dividing and non-dividing cells, long-term persistence and the capacity to accommodate large molecules of foreign DNA. In particular, the natural tropism of herpes virus to infect postmitotic neurons is an advantage that overcomes the difficulty to transfect these cells. In this report, we describe an amplicon that efficiently expresses aequorin targeted to the ER (pHSVerAEQ) in a variety of cell lines and non dividing primary cells, in particular anterior pituitary cells (AP), chromaffin cells and granule neurons. The correct subcellular aequorin location was established by immunocytochemistry and by direct displaying of Ca-sensitive luminescence in each infected cell type. Our results show that delivery of recombinant aequorin to the ER using HSV amplicon is a simple and efficient method to monitor directly $[Ca^{2+}]_{er}$ in adult primary cells such as AP cells, chromaffin and neurons, as well as in several cell lines in culture.

MATERIALS AND METHODS

Cell culture

NIH3T3, wild type HeLa cells and the erAEQmut-HeLa cell clone EM26 [1] were grown in DMEM supplemented with 10% FCS, 2 mM glutamine, 100 U/ml penicillin and 100 mg/ml streptomycin. The 2-2 cell line which contains the HSV-1 IE2 gene [16] was grown in the same medium. PC12 and GH_3 cells were maintained in DMEM with 10% fetal calf serum and 5% horse serum. Anterior pituitary (AP) cells were isolated from adult rats as previously described [17]. Bovine adrenal chromaffin cells were kindly provided by Prof. Antonio García, Universidad Autónoma de Madrid, Spain [18]. Cerebellar granule cells were prepared from 4–7 day-old rats as previously reported [19].

Expression of aequorin in cell cultures using defective HSV vectors

Plasmid construction

The chimeric low-affinity mutant of aequorin erAEQmut has been described previously [1]. The erAEQmut cDNA was isolated from the original vector by EcoRI digestion and cloned into the recipient vector pHSVpuc [20] to generate the pHSVerAEQ. The pHSVlac amplicon vector which expresses the β-galactosidase gene of *Escherichia coli* has been described previously [21].

Packaging of HSV-1 vectors

pHSVerAEQ DNA was packaged into HSV-1 particles using a deletion mutant packaging system [22]. In brief, 3×10^5 2-2 cells were seeded on 60 mm dishes and transfected with 6 μg of pHSVerAEQ or pHSVlac using the lipofectamine procedure according to the manufacturer's protocol (Gibco, BRL, Madrid, Spain). One day later the medium was replaced with 3 ml DMEM, 5% FBS and cells were infected with $\sim 2 \times 10^6$ plaque-forming units of 5dl1.2 helper virus which contains a deletion in the IE2 gene of HSV-1 strain KOS [23]. On the following day, virus was harvested and subsequently passaged on fresh 2-2 cells 3 times to increase both the ratio of vector to helper and the total amount of virus.

Vector titering

Titers were measured in PC12 as described previously [22]. Cells were seeded into poly-L-lysine coated 24-well plates at 5×10^5 cells/well. The next day, cells were infected with various dilutions of each virus and 24 h later the cells were fixed in 4% paraformaldehyde for 30 min. pHSVlac infected cells were detected as previously described [24]. pHSVerAEQ infected cells were visualized by using a mouse anti-HA1 primary antibody 1:200 (Boehringer, Germany) followed by an AP-conjugated anti-mouse secondary antibody (Sigma, Spain). Alkaline phosphatase was visualized using nitroblue tetrazolium and 5-bromo-4-chloro-3-indolyl phosphate according to the manufacturer's instructions (Sigma, Spain). Stained

cells were counted by microscopy and titers of infectious particles were calculated. Titers of vector were expressed as infectious vector particles (ivp) per ml.

Infection of cell cultures

To assay for the capability of the HSV viruses to infect the different cell types, cultures were first infected with pHSVlac. Cells were seeded at semiconfluency onto a 13 mm coverslip and infected 24 h prior to experiments. HeLa cells and NIH3T3 mouse fibroblasts were infected with 1.2×10^4 ivp/ml. PC12, GH_3 and AP cells were infected with 4.8×10^4 ivp/ml, chromaffin cells with 3.6×10^4 ivp/ml and granule cells with 7.2×10^4 ivp/ml. Using an antibody against HA1 we routinely observed a range between 5–30% of cells expressing aequorin. Control experiments were performed to test for cytotoxicity by comparing the effect of extracellular agonists on $[Ca^{2+}]_c$ in both infected and non infected PC12 cells (see below, Fig. 4B). Moreover, measurements of catecholamine secretion from infected bovine chromaffin cells stimulated with caffeine or 70 mM K^+ were virtually identical to the ones obtained in uninfected cells (P. Michelena and A. Garcia, unpublished data). Judging from these two functional analyses, viral infection did not produce significant cytotoxicity in the tested cell types.

Immunofluorescence

Cells were fixed 24 h after infection with 4% paraformaldehyde in PBS for 20 min, washed twice with PBS and once with TBS (100 mM Tris-HCl pH 7.5, 150 mM NaCl). Cells were then blocked for 5 min in TST (0.1% Triton X-100, 1% FCS in TBS) and incubated with the anti-HA1 monoclonal antibody 12CA5 (Boehringer, dilution 1:200) diluted in TST overnight at 4°C. After two washes in TBS, samples were incubated with anti-mouse IgG antibody FITC conjugated (dilution 1:200) for 1–4 h at room temperature. Fluorescence was analyzed routinely with a Nikon Diaphot microscope. Confocal microscopy analysis was performed in a Zeiss LSCM 310 apparatus with a 488 nm band. In the $[Ca^{2+}]_c$ experiments performed in the infected PC12 cells (Fig. 4B), an abbreviated immunofluorescence protocol was carried out at the end of the $[Ca^{2+}]_c$ measurements [25].

$[Ca^{2+}]_{er}$ measurements

Cells were seeded onto 13 mm poly-L-lysine-treated glass coverslips and infected 24 h prior to the experiments. Before reconstituting aequorin, $[Ca^{2+}]_{er}$ was reduced by incubating the cells for 10 min at 37°C with the sarcoplasmic and endoplasmic reticulum Ca^{2+}-ATPase (SERCA) inhibitor 2,5-di-*tert*-butyl-benzohydroquinone

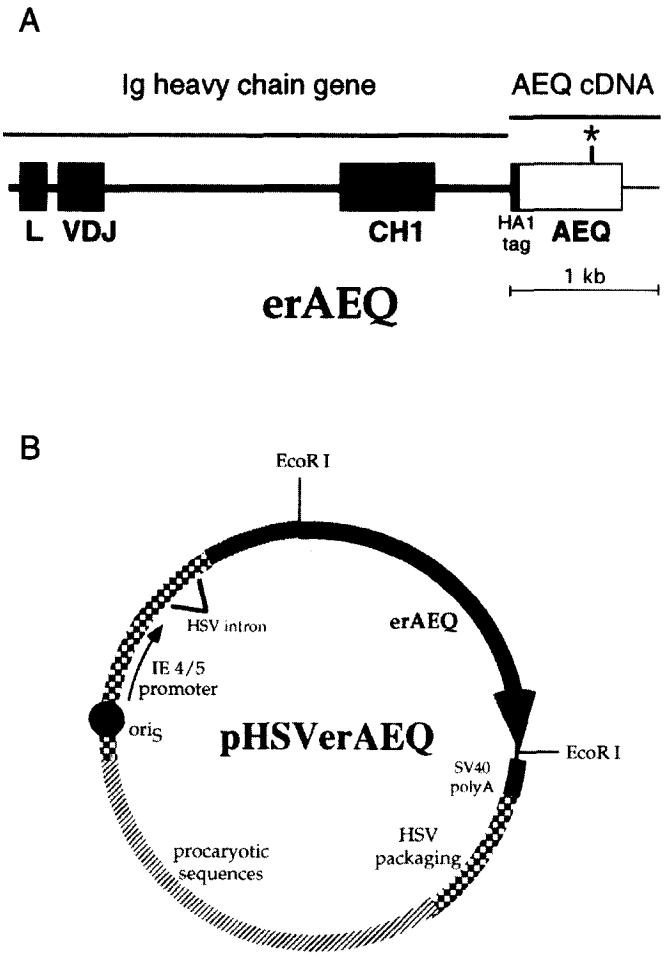

Fig. 1 (**A**) Schematic map of the chimeric erAEQ cDNA. In the Ig moiety, coding and intronic regions are represented by shaded boxes and thick lines, respectively; in the aequorin moiety, coding and non-coding sequences are indicated by a white box and a thin line, respectively. The short sequence encoding the HA1 tag and the point mutation (Asp119 → Ala, asterisk) are indicated. (**B**) Schematic diagram of the amplicon pHSVerAEQ plasmid. The transcriptional unit contains the IE 4/5 promoter, the erAEQ chimeric gene and a polyadenylation signal. Two genetic elements from HSV-1, the *ori*$_s$ and the HSV packaging sequences, allow replication and packaging of the amplicon. The prokaryotic sequences contain a bacterial origin of replication and an ampicillin selection marker that allow propagation and amplification in *E. coli*. A similar vector, carrying the *E. coli lacZ* gene in place of erAEQ was used as a control.

(BHQ) 10 μM in KRB (Krebs-Ringer modified buffer: 125 mM NaCl, 5 mM KCl, 1 mM Na_3PO_4, 1 mM $MgCl_2$, 5.5 mM glucose, 20 mM HEPES, pH 7.4) supplemented with 3 mM EGTA. Cells were then incubated for 1 h at room temperature in KRB containing 0.5 mM EGTA, 10 μM BHQ and 0.5 mM coelenterazine n. The coverslip was then washed for 5 min in KRB containing 0.5 mM EGTA, 5% bovine serum albumin and 10 μM BHQ, and finally placed in the perfusion chamber of a purpose-built thermostated luminometer. Experiments were performed either at 37°C

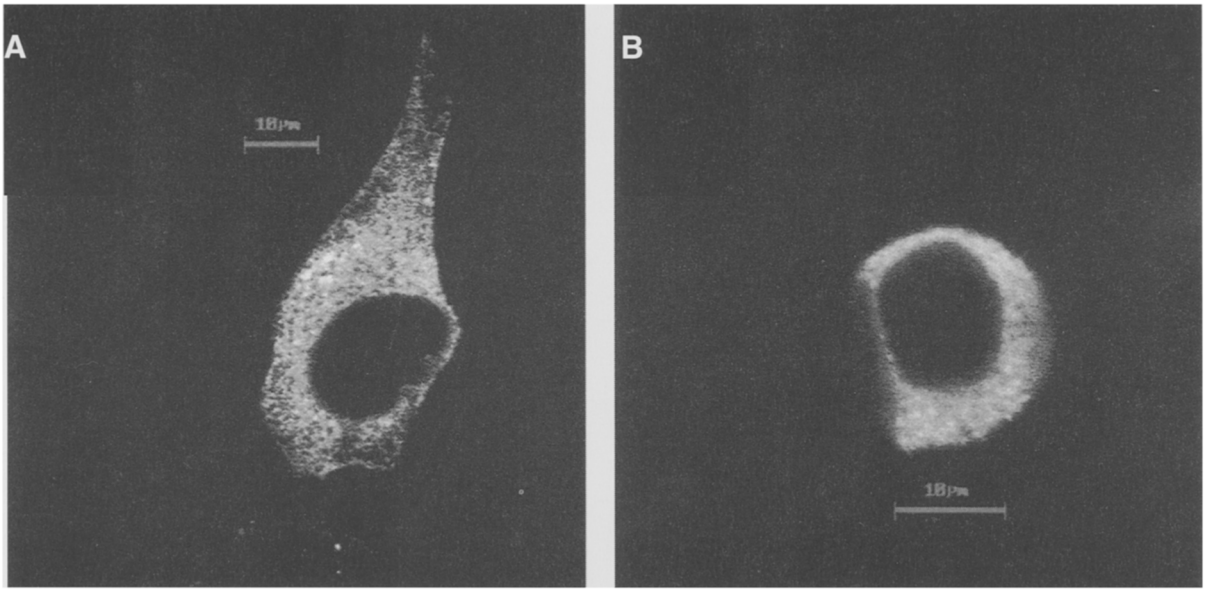

Fig. 2 Immunolocalization of the erAEQ in the infected cells. Confocal images of HeLa cells (**A**) and GH_3 pituitary cells (**B**) infected with the pHSVerAEQ virus 24 h prior to the staining with the anti-HA1 antibody revealed with an FITC-labeled anti-mouse secondary antibody.

or at 22°C. $[Ca^{2+}]_{er}$ values were calculated from the luminescence records using an algorithm which follows the calibration curves previously reported [2,9,14].

$[Ca^{2+}]_c$ measurements

The cells were seeded onto 12 mm poly-L-lysine treated coverslips and infected 24 h prior to the experiments. Cells were loaded with 4 μM Fura–2 and single-cell $[Ca^{2+}]_c$ measurements and time-resolved digital image analysis were performed as previously described [25].

RESULTS

Production of pHSVerAEQ virus and expression of targeted aequorin

The structure of the chimeric cDNA coding for aequorin targeted to the ER has been previously described [1] and is depicted in Figure 1A. This chimera results from the fusion of aequorin with the C-terminus of several domains of the Igγ2b heavy chain responsible for targeting the gene to the ER. The construct also includes an HA1 epitope tag to allow detection by immunocytochemistry and aequorin cDNA carries a mutation (Asp119 → Ala) in one of the three Ca^{2+} binding sites to reduce the affinity for Ca^{2+} of the photoprotein. The pHSVerAEQ plasmid vector is shown schematically in Figure 1B. The erAEQ chimeric construct is cloned in the *EcoRI* site into the pHSVpuc amplicon [20] under the control of the HSV-1 IE (immediate early gene) 4/5 promoter and then packaged into virus particles as outlined in Materials and methods.

In order to verify the correct expression and localization of the targeted protein delivered by the viral vector, cell cultures were infected with the pHSVerAEQ virus and the transduced protein was detected by immunochemistry using a monoclonal antibody to the HA1 epitope of the aequorin moiety. Figure 2 shows the confocal fluorescence images of aequorin distribution in two representative cell types: HeLa (Fig. 2A) and pituitary GH_3 cells (Fig. 2B). The images show a clear perinuclear reticulate staining extending to the periphery of the cell which is characteristic of a protein localized in the ER. Similar patterns of localization were observed in the rest of the studied cell types (data not shown). Detailed evidence showing that the expressed erAEQ fusion protein localizes specifically in the lumen of the ER has been reported previously in HeLa cells, first from studies of colocalization with the ER marker ERp72 [1] and more recently from electron microscopy studies [13].

Functional measurements in cell lines

To investigate whether the expressed aequorin was fully functional, we measured changes in the $[Ca^{2+}]_{er}$ in infected HeLa cells and compared them with those obtained using a stable transfected clone of HeLa cells (clone EM26, [1]) expressing the same chimeric aequorin cloned in the mammalian expression vector pcDNA under the control of the cytomegalovirus promoter. Figure 3 shows the time course of Ca^{2+} reloading and release of the ER in pHSVerAEQ infected HeLa cells (Fig. 3A) and in the HeLa EM26 clone (Fig. 3B). Both cell types were depleted of Ca^{2+} and reconstituted with coelenterazine n as described in

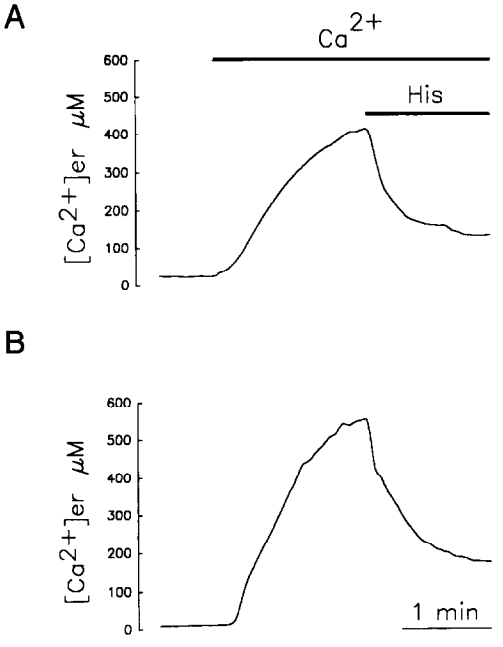

Fig. 3 Comparison between the effect of histamine on $[Ca^{2+}]_{er}$ in pHSVerAEQ-infected HeLa cells (**A**) and in the HeLa EM26 clone (**B**). Wild type HeLa cells were infected with 1.2×10^4 ivp/ml 24 h prior to measurements. Both cells were depleted of Ca^{2+} and reconstituted with coelenterazine n for 1 h prior to measurements. Where indicated, medium containing either only 1 mM $CaCl_2$ (Ca^{2+}) or with 100 μM histamine (His) was perfused. Measurements were performed at 37°C. The total luminescence counts per coverslip were $0.36 \pm 0.13 \times 10^6$ counts/s (cps, $n = 3$) in (A) and $12.8 \pm 1.1 \times 10^6$ cps ($n = 17$) in (B). These experiments are representative of at least 3 similar ones.

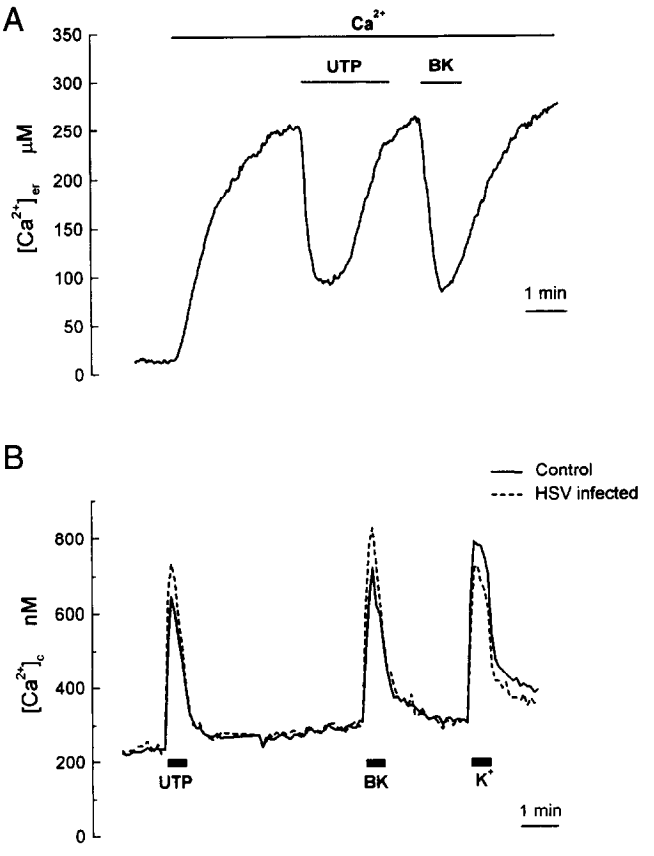

Fig. 4 Effects of UTP, bradykinin (BK) and high K^+ on $[Ca^{2+}]_{er}$ (**A**) and $[Ca^{2+}]_c$ (**B**) in pHSVerAEQ-infected PC12 cells. Cells were infected with 4.8×10^4 ivp/ml 24 h prior to measurements, depleted of Ca^{2+} and either reconstituted with coelenterazine n (for measuring $[Ca^{2+}]_{er}$, A) or loaded with Fura—2 (for measuring $[Ca^{2+}]_c$, B). 100 μM UTP, 1 μM bradykinin and 70 mM K^+ were added when indicated. In (B), an immunofluorescence assay using the anti-HA1 antibody was carried out 'on line' at the end of the $[Ca^{2+}]_c$ measurements to identify the infected cells. The solid line is the average of 57 control (non-infected) cells and the dashed line the average of 10 infected cells in the same microscope field. The $[Ca^{2+}]_c$ increments (measured at the $[Ca^{2+}]_c$ peak) were (mean ± SE): 435 ± 24 nM (control) compared to 531 ± 73 nM (infected) for UTP; 452 ± 17 nM (control) and 575 ± 46 nM (infected) for BK; and 519 ± 20 nM (control) compared to 430 ± 62 nM (infected) for high K^+. The total luminescence counts per coverslip were $1.86 \pm 0.63 \times 10^6$ cps ($n = 5$). These experiments are representative of at least 3 similar ones.

'Materials and methods'. The addition of 1 mM extracellular Ca^{2+} produced a smooth increase in $[Ca^{2+}]_{er}$ leading to a steady-state of 540 ± 40 μM (mean ± SD, $n = 3$) within 2 min in the pHSVerAEQ infected HeLa cells (Fig. 3A). This value of $[Ca^{2+}]_{er}$ was very similar to 550 ± 70 μM ($n = 45$, [2]), obtained in the EM26 clone (Fig. 3B). A subsequent challenge with 100 μM histamine evoked an immediate decrease of $[Ca^{2+}]_{er}$ in both cell types with similar kinetics. Histamine is known to mobilize intracellular Ca^{2+} via generation of $InsP_3$ in these cells [26]. Although the total aequorin luminescence was much lower in the infected HeLa cells than in the stable clone (see figure caption), the calibrated signal showed no significant differences between the dynamics of $[Ca^{2+}]_{er}$ in both types of cells. A similar pattern of $[Ca^{2+}]_{er}$ response was obtained when the related fibroblast cell line NIH3T3 was infected (data not shown).

Rat pheochromocytoma PC12 cells are a neurosecretory cell line very frequently used as a nerve cell model because they share a variety of properties with neurons. Cell cultures were exposed to UTP and bradykinin, agonists coupled to polyphosphoinositide hydrolysis through the P2x puriceptor [27] and the B2 receptor [28], respectively. Figure 4 shows the results obtained in PC12 cells infected with pHSVerAEQ 24 h prior to the measurements. The steady-state level of $[Ca^{2+}]_{er}$ was 370 ± 70 μM ($n = 3$) and addition of 100 μM UTP triggered a very rapid Ca^{2+} release (Fig. 4A). $[Ca^{2+}]_{er}$ returned to the level prior to stimulation within 2 min and subsequent stimulation with 1 μM bradykinin (BK) produced a further reversible decrease in $[Ca^{2+}]_{er}$. These findings are consistent with the results in Figure 4B

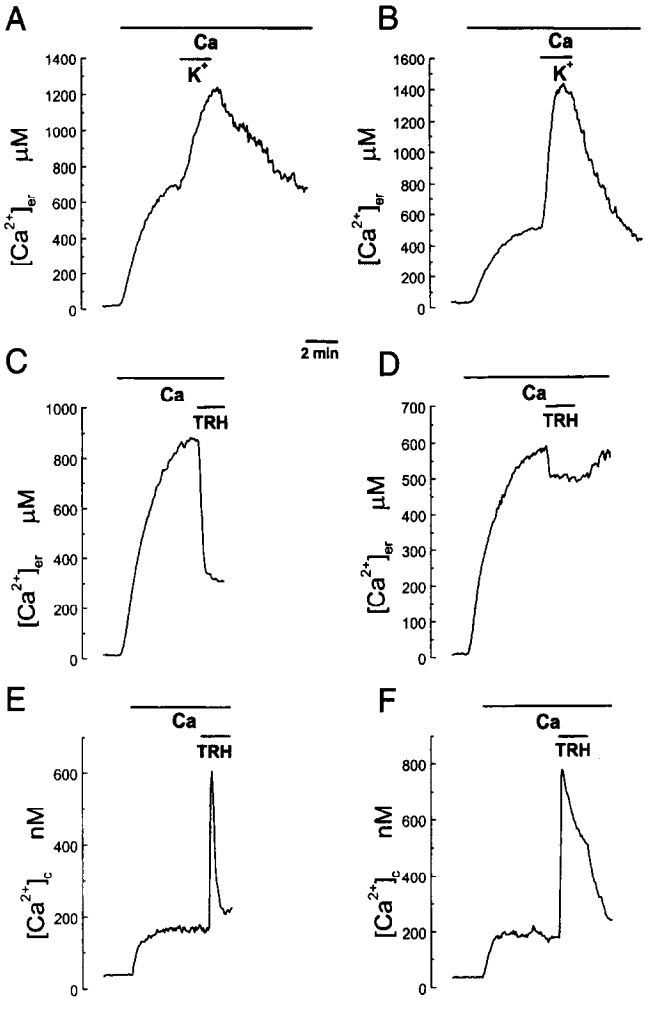

Fig. 5 Effects of high K^+ and TRH on $[Ca^{2+}]_{er}$ and $[Ca^{2+}]_c$ in pHSVerAEQ-infected GH_3 cells (**A,C,E**) and AP cells (**B,D,F**). Cells were infected with 4.8×10^4 ivp/ml 24 h prior to measurements, depleted of Ca^{2+} and either reconstituted with coelenterazine n (for measuring $[Ca^{2+}]_{er}$, **A–D**) or loaded with Fura—2 (for measuring $[Ca^{2+}]_c$, **E** and **F**). The ER was refilled by incubation with 1 mM $CaCl_2$ (Ca) and either 50 mM K^+ (**A** and **B**) or 100 nM TRH (**C–F**) were added when indicated. The total luminescence counts per coverslip were $0.98 \pm 0.09 \times 10^6$ cps ($n = 18$) for GH_3 cells and $0.68 \pm 0.10 \times 10^6$ cps ($n = 19$) for AP cells. Traces (**E**) and (**F**) represent the average of 67 GH_3 and 57 AP cells, respectively, present in the same microscope field. All the measurements were performed at 22°C. Each experiment is representative of at least 3 similar ones.

showing the cytosolic Ca^{2+} increase by the same concentrations of UTP and bradykinin in Fura–2 loaded PC12 cells. Depolarization with high K^+ (70 mM) also elicited a $[Ca^{2+}]_c$ rise. In this figure, the $[Ca^{2+}]_c$ responses in control cells (average of 57 cells, solid line) and in infected cells (average of 10 cells, dashed line) are also directly compared. The infected cells were identified by immunofluorescence at the end of the experiment in the same microscope field used for the Ca^{2+} imaging experiment (*see* 'Materials and methods'). Both the maximal value and the integrated area under the peak for each agonist were not significantly different in control and infected cells. These results indicate that the transduced aequorin was fully functional and that viral infection did not modify functional parameters such as agonist-induced Ca^{2+} release, suggesting that Ca^{2+} regulation was essentially unaltered in pHSVerAEQ infected cells.

Functional measurements in primary cells

To exploit the capacity of herpes virus to infect a wide range of cells, we next expressed targeted aequorin and measured $[Ca^{2+}]_{er}$ in different primary culture cells. Most of the experiments were carried out at 22°C because the rate of aequorin consumption at this temperature is one order of magnitude lower than at 37°C, and this allows monitoring $[Ca^{2+}]_{er}$ during longer times [14].

Pituitary cells are a model for studying the stimulus-secretion coupling of pituitary hormones. They respond to thyrotropin-releasing hormone (TRH) with a rapid increase in $[Ca^{2+}]_c$ due both to release of Ca^{2+} from intracellular stores and to stimulated Ca^{2+} influx from the extracellular medium [29]. They possess voltage-dependent Ca^{2+}-channels that activate on depolarization of the plasma membrane, producing a fast peak in cytosolic Ca^{2+} [17,25]. In Figure 5 we compared the effects of both TRH and depolarization with 50 mM K^+ on $[Ca^{2+}]_{er}$ and $[Ca^{2+}]_c$ in the GH_3 rat pituitary cell line (Fig. 5A,C,E) and in primary AP cells (Fig. 5B,D,F), from which the cell line GH_3 derives. Both cell types were infected with pHSVerAEQ virus during 24 h. Cells were depleted of Ca^{2+} as described in Materials and methods and then reloaded by addition of 1 mM extracellular Ca^{2+} as indicated in the figure. $[Ca^{2+}]_{er}$ increased smoothly during 4–5 min and reached a steady-state at 780 ± 70 μM and 600 ± 150 μM in GH_3 and AP cells (mean ± SD, n = 7), respectively. Depolarization with 70 mM KCl induced a similar response in both pituitary cultures, resulting in a rapid overshoot of $[Ca^{2+}]_{er}$ from 780 μM up to about 1.3 mM in GH_3 cells (Fig. 5A) and near 1.5 mM in primary AP cultures (Fig. 5B). In contrast, stimulation with TRH resulted in a rapid and sustained decrease of $[Ca^{2+}]_{er}$ (by 470 ± 150 μM, $n = 3$) in GH_3 cells (Fig. 5C), but only in a minor decrease in $[Ca^{2+}]_{er}$ of around 70 μM in AP cells (Fig. 5D). The small Ca^{2+} response to TRH observed in AP cells cannot be attributed to inhibition of Ca^{2+} release by cytosolic Ca^{2+}, as found for HeLa cells [2,14], because loading the cells with BAPTA did not modify the effect of TRH on $[Ca^{2+}]_{er}$ (data not shown). In contrast to this striking difference in the $[Ca^{2+}]_{er}$ responses, measurements of $[Ca^{2+}]_c$ in GH_3 (Fig. 5E) and AP cells (Fig. 5F) loaded with Fura–2 and stimulated with TRH showed very similar responses. In both cases, most of the individual cells (50–75%) responded to TRH with a fast and transient $[Ca^{2+}]_c$

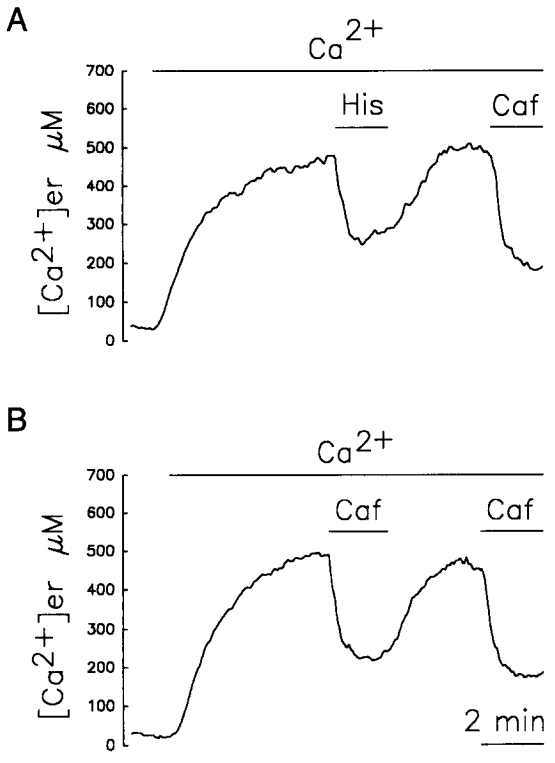

Fig. 6 Effects of histamine and caffeine on $[Ca^{2+}]_{er}$ in pHSVerAEQ-infected bovine chromaffin cells. Cells were infected with 3.6×10^4 ivp/ml 24h prior to measurements. (**A**) 10 μM histamine (His) or 10 mM caffeine (Caf) was added when indicated. (**B**) Two pulses of 10 mM caffeine were added as indicated. The total luminescence counts per coverslip were $1.05 \pm 0.16 \times 10^6$ cps ($n = 14$). Other details as in Figure 3. These experiments are representative of at least 3 similar ones.

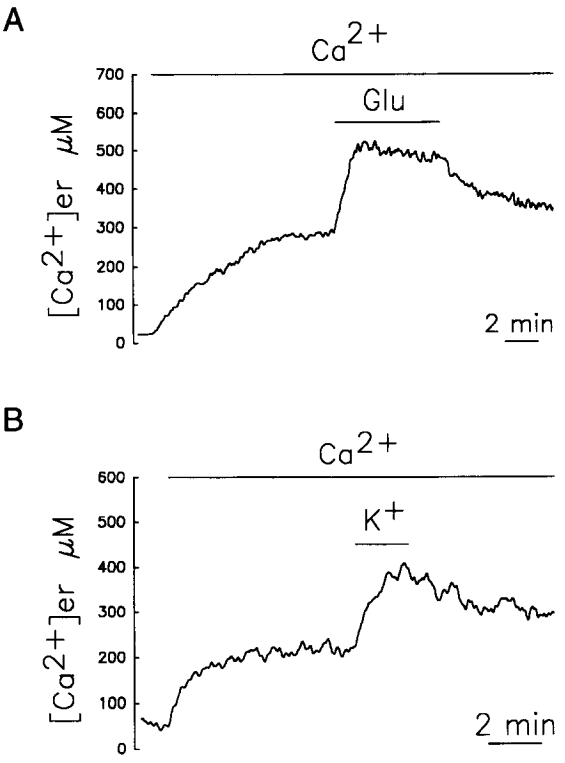

Fig. 7 Effects of glutamate (Glu) and high K^+ on $[Ca^{2+}]_{er}$ in pHSVerAEQ-infected cerebellar granule cells. Cells were infected with 7.2×10^4 ivp/ml 24 h prior to measurements. 100 μM glutamate (**A**) and 50 mM K^+ (**B**) were added as indicated. The total luminescence counts per coverslip were $0.19 \pm 0.07 \times 10^6$ cps ($n = 4$). Other details as in Figure 3. These experiments are representative of at least 3 similar ones.

increase. The average increase of $[Ca^{2+}]_c$ at the peak was about 600–800 nM in both cell types.

One of the main advantages of the HSV amplicon system is the ability to infect non-dividing cells such as neurons. This allows using the pHSVerAEQ virus to study the dynamics of neuronal Ca^{2+} stores. In this report, we have employed two different cell types: chromaffin and cerebellar granule cells. Adrenal medulla chromaffin cells can be regarded as a highly specialized form of post-ganglionic sympathetic neurons. They derive embryologically from the neural crest, are electrically excitable and release vesicle-contained substances in response to specific stimuli. They are frequently utilized in studies on CICR mechanisms and the relationship between $InsP_3$- and ryanodine-sensitive stores. Here, we have used histamine to activate the $InsP_3$-sensitive Ca^{2+} release mechanism and caffeine to activate the CICR mechanism present in these cells [30]. Figure 6 shows the results obtained in pHSVerAEQ infected bovine chromaffin cells. The addition of 1 mM Ca^{2+} to Ca^{2+}-depleted chromaffin cells induced an elevation of the $[Ca^{2+}]_{er}$ up to a steady-state of 650 ± 100 mM ($n = 13$) within 4–5 min (Fig. 6A). Subsequent exposure to 10 μM histamine triggered a rapid decrease of $[Ca^{2+}]_{er}$ to about 60% of the initial level. After washing out the agonist, the ER reloaded with Ca^{2+} up to the same steady-state, and the cells responded to a latter application of 10 mM caffeine with a second drop in $[Ca^{2+}]_{er}$. A similar pattern was obtained, both in time course and amplitude, when the cells were challenged with two consecutive pulses of 10 mM caffeine (Fig. 6B). These data indicate that two different stimuli, acting either via $InsP_3$ receptors or via ryanodine receptors, are able to release comparable amounts of Ca^{2+} from the ER in chromaffin cells.

Finally, a primary postmitotic neuronal culture was used. We delivered the targeted aequorin into rat cerebellar granule cells by infecting them with the pHSVerAEQ virus. Figure 7 illustrates a representative example in which granule cells were stimulated either with glutamate or with 50 mM K^+. The steady-state level of $[Ca^{2+}]_{er}$ was 300 ± 60 μM ($n = 3$), somewhat lower than in the other cell types studied. Addition of 100 μM

glutamate (Fig. 7A) elicited an increase in $[Ca^{2+}]_{er}$ followed by a slow decline accelerated by removal of the agonist. Metabotropic glutamate receptor agonists like quisqualate (1 μM) and *trans*-1-aminocyclopentane-1S,3R-dicarboxylic acid, (*trans*-ACPD, 100 μM) did not induce any significant change in the $[Ca^{2+}]_{er}$ level (data not shown). This result is consistent with the lack of effect of these agonists on $[Ca^{2+}]_c$ in single cell imaging experiments in our granule cell cultures (data not shown). Finally, a 2 min depolarization pulse with 50 mM K^+ (Fig. 7B) also induced an increase in the $[Ca^{2+}]_{er}$ signal very similar to that evoked by glutamate.

DISCUSSION

Considerable interest is presently focused on the dynamics of $[Ca^{2+}]_{er}$ due to its role as the main reservoir of Ca^{2+}, able to be rapidly released into the cytosol upon cell stimulation. However, the estimates of the steady-state $[Ca^{2+}]_{er}$ reported in the literature have been conflicting, probably because of the different methodologies used [31]. Many of the measurements were undertaken with low-affinity fluorescent probes, which have important limitations such as non-specific localization throughout the cell and interference with Mg^{2+}. In fact, due to the need to eliminate the strong dye signal arising from the cytosol, most of these studies have been performed in permeabilized, quenched or patched cells [32,33]. Several of these problems can be overcome using ER-targeted photoproteins. They are specifically localized in the ER, thus allowing selective monitoring of lumenal $[Ca^{2+}]_{er}$ changes in intact cells. Furthermore, aequorin does not display Mg^{2+}-sensitive luminescence and it has a greater dynamic range than fluorescent dyes. However, the first attempts to measure $[Ca^{2+}]_{er}$ using ER-targeted aequorin turned out to be particularly difficult because of the rapid aequorin consumption resulting from the high $[Ca^{2+}]$ present in this compartment. Thus, not only the wild type [10,11], but also the low-affinity version of aequorin are endowed with a Ca^{2+} affinity too high to reliably measure $[Ca^{2+}]_{er}$ [1,13]. We have recently solved this problem by using coelenterazine n, a chemically modified form of the prosthetic group that reduces the rate of luminescence, thus allowing measurements of steady-state $[Ca^{2+}]_{er}$ around 500 μM in HeLa cells [2,14]. These results were in close agreement with data recently reported, also in HeLa cells, using an ER-targeted chimera dubbed 'cameleon' (34). The authors found that 90% of the cell population had $[Ca^{2+}]_{er}$ at steady state around 400 μM [35]. The steady-state $[Ca^{2+}]_{er}$ estimated here in the different cell types studied were also in the same range, from 300 μM in granule cells to 800 μM in GH_3 cells.

Up to now, studies of the dynamics of $[Ca^{2+}]_{er}$ using ER-targeted constructs (aequorin- or cameleon-based) have been mostly performed in adherent cell lines (particularly HeLa cells) and very limited information is available for primary adult cells. The reason is that non-dividing cells are refractory to the more common methods of introduction of DNA like Ca^{2+} phosphate. Herpes viral vectors are a powerful tool for gene transfer into postmitotic cells and, more specifically, into adult neurons. Moreover, HSV-1 can efficiently infect a wide variety of established lines of diverse origin, thus overcoming many of the limitations concomitant to DNA transfection or the selection of a stable transfected clone. Given the physiological relevance of the Ca^{2+} stores in primary excitable cells, we decided to exploit the wide host range of the HSV-1 system to deliver the ER-targeted aequorin to a number of different cell types. Thus, we have generated a replication deficient herpes simplex type 1 virus containing the ER-targeted low affinity aequorin gene (pHSVerAEQ). Viral infection of both primary postmitotic cells and established cell lines led to the correct expression of the chimeric aequorin selectively into the lumen of the ER as determined by immunostaining and by functional $[Ca^{2+}]_{er}$ studies. The transduced chimeric ER-targeted aequorin displayed Ca^{2+}-sensitive luminescence and could be easily used to monitor $[Ca^{2+}]_{er}$ changes elicited by $InsP_3$-generating agonists, caffeine and activation of voltage-gated or receptor-operated Ca^{2+} channels in a variety of cells. The data presented here are the first report of direct measurements of the dynamics of $[Ca^{2+}]_{er}$ in pituitary cells (both GH_3 and AP cells), PC12, chromaffin and cerebellar granule cells. The use of an adenovirus vector to target wild type aequorin to the ER has been recently reported [36]. However, although the authors showed expression of the apoprotein in the ER of the infected cells, no measurements of $[Ca^{2+}]_{er}$ were provided. As we have already discussed, wild type aequorin reconstituted with native coelenterazine cannot provide reliable measurements of $[Ca^{2+}]_{er}$ due to the rapid consumption of the probe [13].

Regarding the physiological data reported in this study, it was surprising to find that TRH produced such a small effect in AP cells compared with that obtained in GH_3 cells (compare Fig. 5D and C), even though the agonist is able to induce a comparable $[Ca^{2+}]_c$ increment in both cell types (compare Fig. 5E and F and see [17,25]). Apparently, a relatively modest mean decrease of about 70 μM in $[Ca^{2+}]_{er}$ is enough to produce a $[Ca^{2+}]_c$ peak of 700 nM in 50–75% of the AP cells analyzed by single cell imaging. This dissociation between the decrease in $[Ca^{2+}]_{er}$ and the $[Ca^{2+}]_c$ peak is in agreement with our previous results in histamine-stimulated HeLa cells, where the changes in $[Ca^{2+}]_{er}$ and $[Ca^{2+}]_c$ were directly compared [2,14]. Those results were interpreted in terms of a strong and rapid inhibition of the $InsP_3$-gated

channels by microdomains of high $[Ca^{2+}]_c$ in the vicinity of the channels. However, experiments designed to test this hypothesis by loading the AP cells with BAPTA prior to TRH stimulation showed no acceleration of the $[Ca^{2+}]_{er}$ drop (data not shown), suggesting that the mechanism may be more complex in this case. In fact, the magnitude of the response of $[Ca^{2+}]_{er}$ to an $InsP_3$-producing agonist appears to be quite variable depending on either the cell or the agonist used. Thus, histamine in chromaffin cells or other $InsP_3$-producing stimuli like UTP or bradykinin in PC12 cells did induce a rapid, large Ca^{2+} release from the ER (see Figs 6A & 4A). In any case, one important conclusion from these results is that there is not always a direct correlation between the height of the $[Ca^{2+}]_c$ peak measured with fluorescence indicators and the amount of Ca released from the ER. For this reason, the content of the stores cannot be estimated accurately from the height of the $[Ca^{2+}]_c$ peak induced by a Ca^{2+}-releasing agonist and direct measurement of $[Ca^{2+}]_{er}$ becomes essential.

Given the natural propensity of herpes virus to infect postmitotic neurons, an immediate application of this technique is to study neuronal Ca^{2+} stores. It has become clear in recent years that intracellular Ca^{2+}-storage sites can play a crucial role in regulating complex Ca^{2+} signals and neuronal responses such as excitability, synaptic plasticity, release of neurotransmitters and perhaps neuronal death [37]. It is well known that stimulation of glutamate receptors in neuronal cells elicits an increase of the $[Ca^{2+}]_c$ due to Ca^{2+} entry through both the NMDA channel complex and other voltage-gated Ca^{2+} channels [38]. Our present results in cerebellar granule cells (see Fig. 7A) show that stimulation with glutamate induces a rapid increase in $[Ca^{2+}]_{er}$, which can be explained from the stimulation of the sarco- and endoplasmic reticulum Ca^{2+}-ATPases (SERCA) by the increase in $[Ca^{2+}]_c$ due to activated Ca^{2+} entry. Although recent results suggest that the ionotropic receptor-mediated $[Ca^{2+}]_c$ signals might also involve release of Ca^{2+} from intracellular stores by CICR [39], our data do not support this hypothesis in cerebellar granule cells. On the other hand, addition of quisqualate, or the more selective metabotropic glutamate receptor agonist *trans*-ACPD, to the neuronal culture did not produce any response either in $[Ca^{2+}]_{er}$ or in $[Ca^{2+}]_c$, suggesting that our cultures of granule cells lack metabotropic glutamate receptors.

Studies in a number of neuronal preparations have indicated that depolarizing stimuli can activate a calcium-induced-calcium-released (CICR) mechanism [39]. However, the involvement of CICR in the generation of $[Ca^{2+}]_c$ peaks has been difficult to estimate due to the parallel activation of plasma membrane Ca^{2+} channels and the subsequent massive Ca^{2+} entry. Speculations on the role of CICR have been quite variable depending on the methodology used to produce depolarization, leading to conflicting results in the literature. In our experimental conditions we did not observe any sign of activation of CICR upon a 2 min pulse with high K^+ medium in GH_3, AP cells or granule neurons (see Figs 5A,B & 7B). Instead, high K^+ depolarization always elicited a significant increase in $[Ca^{2+}]_{er}$ in all cells tested. Again, the most probable explanation for this effect is the stimulation of the SERCA by the increase in $[Ca^{2+}]_c$. Another tool often used to examine the role of CICR is the ability of caffeine to elicit release of intracellular Ca^{2+}. Our measurements of $[Ca^{2+}]_{er}$ in adrenal chromaffin cells (Fig. 6) confirm that caffeine mobilizes Ca^{2+} from the intracellular stores in these cells, a result consistent with earlier reports using fluorimetric techniques to measure $[Ca^{2+}]_c$ [30,40].

In conclusion, the data presented here demonstrate that the HSV based technology is an efficient method to deliver the ER-targeted aequorin to a number of mammalian cells, both established lines and postmitotic primary cells. Future developments may include producing new HSV vectors carrying aequorin chimeras targeted to other compartments (e.g. nucleus, mitochondria) or expressing other targeted indicator genes such as the recently reported cameleons [34] that allow performing single-cell imaging experiments. This approach will facilitate the study of key physiological issues such as the role of neuronal calcium stores or the behavior of functionally distinct Ca^{2+} pools within the ER.

ACKNOWLEDGEMENTS

We are indebted to Dr F. Lim for helping us to establish the HSV mediated gene transfer technique in our laboratory and for his ever present advise on the amplicon system. We thank P. Alarcón for help with the imaging experiments and both P. Alarcón and Dr A. Sanchez for generously providing AP cells. We acknowledge Dr P. Michelena and Dr A. Garcia for chromaffin cells. We also thank J. Fernandez for technical assistance. We are grateful to S. Calleja for assistance with confocal microscopy. We specially thank Dr T. Schimmang for his helpful comments on the manuscript. This research was supported by grants from Spanish Government Agencies for Health Research FIS 96/1443 (MTA), FIS 96/0456 (JA) and DGICYT PB92/0268 (JG-S) and fellowships to MJB and EC.

REFERENCES

1. Montero M., Brini M., Marsault R. et al. Monitoring dynamic changes in free Ca^{2+} concentration in the endoplasmic reticulum of intact cells. *EMBO J* 1995; **14**: 5467–5475.
2. Montero M., Barrero M.J., Alvarez J. [Ca^{2+}] microdomains control agonist-induced Ca^{2+} release in intact cells. *FASEB J* 1997; **11**: 881–886.
3. Bootman M.D., Berridge M.J. The elemental principles of calcium signaling. *Cell* 1995; **83**: 675–678.

4. Berridge M.J. Inositol trisphospate and calcium signaling. *Nature* 1993; **361**: 315–325.
5. Clapham D.E. Calcium signaling. *Cell* 1995; **80:** 259–268.
6. Pozzan T., Rizzuto R., Volpe P., Meldolesi J. Molecular and cellular physiology of intracellular calcium stores. *Physiol Rev* 1994; **74**: 595–636.
7. Rizzuto R., Simpson A.W.M., Brini M., Pozzan T. Rapid changes of mitochondrial Ca^{2+} revealed by specifically targeted recombinant aequorin. *Nature* 1992; **358**: 325–328.
8. Brini M., Murgia M, Pasti L., Picard D., Pozzan T., Rizzuto R. Nuclear Ca^{2+} concentration measured with specifically targeted recombinant aequorin. *EMBO J* 1993; **12**: 4813–4819.
9. Brini M., Marsault R., Bastianutto C., Alvarez J., Pozzan T., Rizzuto R. Transfected aequorin in the measurement of cytosolic Ca^{2+} concentration $[(Ca^{2+})]_c$: a critical evaluation. *J Biol Chem* 1995; **270:** 9896–9903.
10. Kendall J.M., Dormer R.L., Campbell A.K. Targeting aequorin to the endoplasmic reticulum of living cells. *Biochem Biophys Res Commun* 1992; **189**: 1008–1016.
11. Button D., Eidsath A. Aequorin targeted to the endoplasmic reticulum reveals heterogeneity in luminal Ca^{2+} concentration and reports agonist- or IP_3-induced release of Ca^{2+}. *Mol Biol Cell* 1996; **7**: 419–434.
12. Brini M., De Giorgi F., Murgia M. et al. Subcellular analysis of Ca^{2+} homeostasis in primary cultures of skeletal muscle myotubes. *Mol Biol Cell* 1997; **8**: 129–143.
13. Montero M., Alvarez J., Scheenen W.J.J., Rizzuto R., Meldolesi J., Pozzan T. Ca^{2+} homeostasis in the endoplasmic reticulum: coexistence of high and low $[Ca^{2+}]$ subcompartments in intact HeLa cells. *J Cell Biol* 1997; **139**: 601–611.
14. Barrero M.J., Montero M., Alvarez J. Dynamics of $[Ca^{2+}]$ in the endoplasmic reticulum and cytosol of intact HeLa cells. A comparative study. *J Biol Chem* 1997; **272**: 27694–27699.
15. Fink D.J., DeLuca N.A., Goins W.F., Glorioso J.C. Gene transfer to neurones using herpes simplex virus-based vectors. *Annu Rev Neurosci* 1996; **19**: 265–287.
16. Smith I.L., Hardwicke M.A., Sandri-Goldin R.M. Evidence that the herpes simplex virus immediate early protein ICP27 acts post-transcriptionally during infection to regulate gene expression. *Virology* 1992; **186**: 74–86.
17. Villalobos C., Nuñez L., Garcia-Sancho J. Functional glutamate receptors in a subpopulation of anterior pituitary cells. *FASEB J* 1996; **10**: 654–660.
18. Moro M.A., Lopez M.G., Gandia L., Michelena P., Garcia A.G. Separation and culture of living adrenaline- and noradrenaline-containing cells from bovine adrenal medullae. *Anal Biochem* 1990; **185**, 243–248.
19. Nuñez L., Sanchez A., Fonteriz R.I., Garcia-Sancho J. Mechanisms for synchronous calcium oscillations in cultured rat cerebellar neurons. *Eur J Neurosci* 1996; **8**: 192–201.
20. Geller A.I., During M.J., Haycock J.W., Freese A., Neve R. Long-term increases in neurotransmitter release from neuronal cells expressing a constitutive active adenylate cyclase from a herpes simplex virus type 1 vector. *Proc Natl Acad Sci USA* 1993; **90**: 7603–7607.
21. Geller A.I., Breakefield X.O. A defective HSV-1 vector expressed *Escherichia coli* beta-galactosidase in cultured peripheral neurons. *Science* 1988; **241**: 1667–1669.
22. Lim F., Hartley D., Starr P. et al. Generation of high-titer defective HSV-1 vectors using an IE 2 deletion mutant and quantitative study of expression in cultured cortical cells. *Biotechniques* 1996; **20**, 460–469.
23. McCarthy A.M., McMahan L., Schaffer P.A. Herpes simplex virus type 1 ICP27 deletion mutants exhibit altered patterns of transcription and are DNA deficient. *J Virol* 1989; **63**: 18–27.
24. Sanes J.R., Rubenstein J.L.R., Nicolas J.F. Use of a recombinant retrovirus to study post-implantation cell lineage in mouse embryos. *EMBO J* 1986; **5**: 3133–3142.
25. Villalobos C., Nuñez L., Frawley L.S., Garcia-Sancho J., Sanchez A. Multi-responsiveness of single anterior pituitary cells to hypothalamic-releasing hormones: a cellular basis for paradoxical secretion. *Proc Natl Acad Sci USA* 1997; **94**, 14132–14137.
26. Bootman M.D., Berridge M.J., Taylor C.W. All or nothing Ca^{2+} mobilization from the intracellular stores of single histamine stimulated HeLa cells. *J Physiol* 1992; **450**: 163–178.
27. Majid M.A., Okajima F., Kondo Y. UTP activates phospholipase C-Ca^{2+} system through a receptor different from the 53-kDa ATP receptor in PC12 cells. *Biochem Biophys Res Commun* 1993; **195**: 415–421.
28. Fasolato C., Pandiella A., Meldolesi J., Pozzan T. Generation of inositol phosphates, cytosolic Ca^{2+} and ionic fluxes in PC12 cells treated with bradykinin. *J Biol Chem* 1988; **263**: 17350–17359.
29. Gershengorn M.C. Mechanisms of thyrotropin-releasing hormone stimulation of pituitary hormone secretion. *Annu Rev Physiol* 1986; **48**: 515–526.
30. Cheek T.R., Moreton R.B., Berridge M.J., Stauderman K.A., Murawsky M.M., Bootman M.D. Quantal Ca^{2+} release from caffeine-sensitive stores in adrenal chromaffin cells. *J Biol Chem* 1993; **268**: 27076–27083.
31. Bygrave F.L., Benedetti A. What is the concentration of calcium ions in the endoplasmic reticulum? *Cell Calcium* 1996; **19**: 547–551.
32. Tse W.F., Tse A., Hille B. Cyclic Ca^{2+} changes in intracellular stores of gonadotropes during gonadotropin-releasing hormone-stimulated Ca^{2+} oscillation. *Proc Natl Acad Sci USA* 1994; **91**: 9750–9754.
33. Hofer A.M., Machen T.E. Technique for in situ measurement of calcium in intracellular inositol 1,4,5-trisphosphate-sensitive stores using the fluorescent indicator mag-Fura–2. *Proc Natl Acad Sci USA* 1995; **90**: 2598–2602.
34. Miyawaki A., Llopis J., Heim R. et al. Fluorescent indicators for Ca^{2+} based on green fluorescent proteins and calmodulin. *Nature* 1997; **388**: 882–887.
35. Pozzan T. Calcium turns turquoise into gold. *Nature* 1997; **388**: 834–835.
36. Kendall J.M., Badminton M.N., Sala-Newby G.B., Wilkinson G.W.G., Campbell A.K. Agonist-stimulated aequorin to organelles using a replication deficient adenovirus vector. *Cell Calcium* 1996; **19**: 133–142.
37. Henzi V., McDermott A.B. Characteristics and function of Ca^{2+} and inositol 1,4,5-trisphosphate-releasable stores of Ca^{2+} in neurons. *Neuroscience* 1992; **46**: 251–274.
38. Gassic G.P., Hollmann M. Molecular neurobiology of glutamate receptors. *Annu Rev Physiol* 1992; **54:** 507–536.
39. Simpson P., Challiss R., Nahorski S. Neuronal Ca^{2+} stores: activation and function. *Trends Neurosci* 1995; **18**: 299–306.
40. Malgaroli A., Fesce R., Meldolesi R. Spontaneous $[Ca^{2+}]_i$ fluctuations in rat chromaffin cells do not require inositol 1,4,5-trisphosphate elevations but are generated by a caffeine- and ryanodine-sensitive intracellular Ca^{2+} store. *J Biol Chem* 1990; **265**: 3005–3008.